Genomics Data 6 (2015) 99–107

Contents lists available at ScienceDirect

Genomics Data

journal homepage: http://www.journals.elsevier.com/genomics-data/

Data in Brief

Defects in cytochrome c oxidase expression induce a metabolic shift to glycolysis and carcinogenesis

Dawei W. Dong [a,b,*], Satish Srinivasan [a], Manti Guha [a], Narayan G. Avadhani [a]

[a] The Department of Biomedical Sciences, School of Veterinary Medicines, University of Pennsylvania, PA, United States
[b] Institute for Biomedical Informatics, Perelman School of Medicine, University of Pennsylvania, PA, United States

ARTICLE INFO

Article history:
Received 29 June 2015
Received in revised form 19 July 2015
Accepted 26 July 2015
Available online 14 August 2015

Keywords:
Genome expression
Functional analysis
Tumor progression
Mitochondrial metabolic dysfunction
Cytochrome c oxidase defects

ABSTRACT

Mitochondrial metabolic dysfunction is often seen in cancers. This paper shows that the defect in a mitochondrial electron transport component, the cytochrome c oxidase (CcO), leads to increased glycolysis and carcinogenesis. Using whole genome microarray expression analysis we show that genetic silencing of the CcO subunit Cox4i1 in mouse C2C12 myoblasts resulted in metabolic shift to glycolysis, activated a retrograde stress signaling, and induced carcinogenesis. In the knockdown cells, the expression of Cox4i1 was less than 5% of the control and the expression of the irreversible glycolytic enzymes (Hk1, Pfkm and Pkm) increased two folds, facilitating metabolic shift to glycolysis. The expression of Ca^{2+} sensitive Calcineurin (Ppp3ca) and the expression of PI3-kinase (Pik3r4 and Pik3cb) increased by two folds. This Ca^{2+}/Calcineurin/PI3K retrograde stress signaling induced the up-regulation of many nuclear genes involved in tumor progression. Overall, we found 1047 genes with 2-folds expression change (with *p*-value less than 0.01) between the knockdown and the control, among which were 35 up-regulated genes in pathways in cancer (enrichment *p*-value less than 10^{-5}). Functional analysis revealed that the up-regulated genes in pathways in cancer were dominated by genes in signal transduction, regulation of transcription and PI3K signaling pathway. These results suggest that a defect in CcO complex initiates a retrograde signaling which can induce tumor progression. Physiological studies of these cells and esophageal tumors from human patients support these results. GEO accession number = GSE68525.

Specifications	
Organism/cell line/tissue	Mus musculus/C2C12 myoblasts
Sequencer or array type	Affymetrix GeneChip Mouse Gene 2.0ST Arrays scanned by Affymetrix GeneChip Scanner 3000
Data format	Raw CEL files and RMA summary
Experimental factors	Tumorigenic vs. control cells
Experimental features	Genetic silencing of Cox4i1 by shRNA induced a tumorigenic phenotype in C2C12 myoblasts, the mRNA expression of which was compared to the control with scrambled shRNA

1. Direct link to deposited data

http://www.ncbi.nlm.nih.gov/geo/query/acc.cgi?acc=GSE68525

2. Direct link to deposited source codes

http://code.vet.upenn.edu/download/CcOdefect/

3. Experimental Design, Materials and Methods

3.1. Sample preparation

Cells were grown in Dulbecco's Modified Eagle medium supplemented with 10% fetal bovine serum and 0.1% penicillin/streptomycin. In case of Cox4i1 silenced (C4KD) cells, the medium was further supplemented with 1 mM Pyruvate and 50 μg/ml Uridine. RNA was prepared using Qiagen Rneasy kit following manufacturer's instructions. 5.5 μg single-stranded cDNA was fragmented and labeled using the Affymetrix GeneChip WT Terminal Labeling kit (PN: 900671). Labeled cDNA (3.25 μg) was hybridized for 17 h at 45°C to Affymetrix GeneChip Mouse Gene 2.0ST Arrays (PN: 902118).

3.2. Microarray analysis

The data were processed by Affymetrix Expression Console using Probeset-Summarize-Engine with default setting of the robust multi-

* Corresponding author at: The Department of Biomedical Sciences, School of Veterinary Medicines, University of Pennsylvania, PA, United States.
E-mail address: ddong@mail.med.upenn.edu (D.W. Dong).

http://dx.doi.org/10.1016/j.gdata.2015.07.031

array average (RMA, [1]) method to calculate the expression level for each probeset of the array (in log_2 unit, online file: rma-gene-full.summary.txt). For quality control, we performed principal component analysis (PCA) based on RMA expression levels of the samples. The projection to the most dominant two components is shown in Fig. 1a. The control samples formed a single cluster separable from the knockdown. However, the knockdown samples are further branched into two groups. The grouping is also clearly shown (Fig. 1b) by the correlation coefficient value (with each probe mean over all samples removed) between two samples: if the two samples come from the same group, the value is high (above 0.6); if they come from different groups, the value is low or negative. Further investigation of the biological samples showed that C4KD1 and C4KD2 cells contained nearly 90% reduced Cox4i1 mRNA and protein as compared to control cells [2], while in C4KD3 cells the reduction was not as much (probably due to a less effective population selection by antibiotic resulting a mixture of knockdown and non-knockdown cells). This is consistent with microarray results: for both C4KD1 and C4KD2 the reduction were ~20 folds, for C4KD3 only ~2 folds. In the following analysis, C4KD3 was excluded.

3.3. Statistical analysis

Fold changes are presented as the mean ± s.e.m. (standard error of the mean) and *p*-values were determined by one-tailed Welch's t-test, which is used to test the hypothesis that two populations have equal means and is more reliable than Student's t-test when the samples from two populations have unequal variances and unequal sample sizes [3]. So for a statistic t and a degrees of freedom v, the p-value is calculated by

$$\frac{1}{2} I_{\frac{v}{v+t^2}}\left(\frac{v}{2},\frac{1}{2}\right) \tag{1}$$

where I is the regularized incomplete beta function. The statistic t is defined by the following formula:

$$t = \frac{m_1 - m_2}{\sqrt{s_1 + s_2}} \tag{2}$$

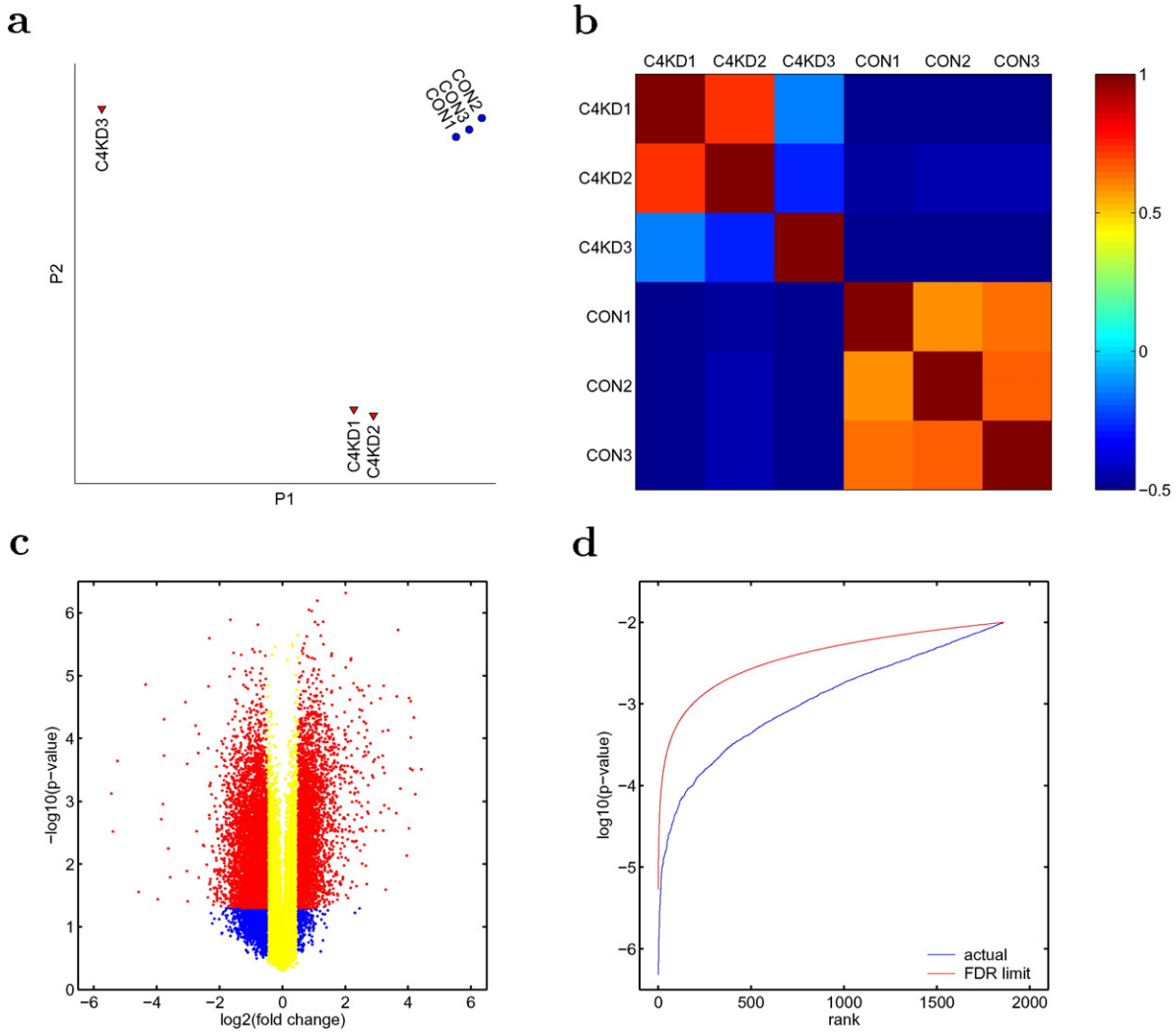

Fig. 1. Quality control for data analysis. The array expression data (from all 41,345 probes) of each sample are projected to the first two components of PCA, P1 and P2 in **a**, showing the separation of 6 samples into three groups. This separation is also shown in the 6×6 matrix of the correlation coefficients between samples (**b**). The plot in (**c**) shows the selection criteria for significant fold change in individual gene expression: the absolute fold change has to be bigger than $2^{0.5}$ (red and blue dots), and the p-value has to be smaller than 0.05. For functional analysis, the selected genes are ranked by p-value and are further selected by Benjamini-Hocheberg method to limit FDR (**d**).

where m_1 and s_1 are the mean and the s.e.m of the 1st sample, and m_2 and s_2 of the 2nd sample. The degrees of freedom v is approximated by

$$v \approx \frac{\left(s_1^2 + s_2^2\right)^2}{\frac{s_1^4}{v_1 - 1} + \frac{s_2^4}{v_2 - 1}} \quad (3)$$

where v_1 and v_2 are the 1st and 2nd sample size, respectively. All calculations are performed using RMA expression levels, i.e., in log_2 unit. For a given gene, a fold change $>2^{0.5}$ with a p-value <0.05 was considered statistically significant. Fig. 1b shows the distribution of fold change versus p-value for the full probeset of the Affymetrix GeneChip Mouse Gene 2.0ST Arrays. Out of 41,345 probes, 6049 had statistically significant fold change (red dots in Fig. 1c). Among those are 4908 uniquely identified genes (out of 26,515 Entrez genes of the array). Each individual gene expression presented in the paper is among those.

3.4. Pathway analysis

The list of genes with significant fold change was uploaded to KEGG Mapper to search pathways (http://www.genome.jp/kegg/tool/map_pathway1.html, [4]). To further narrow down the list of pathways, we calculated the p-value of pathway enrichment. With H the hits, i.e., the number of genes from our list present in a pathway of size S, N the number of genes of the list, and T the total number of genes of the array, the enrichement p-value was determined by

$$1 - F(H-1; T, S, N) \quad (4)$$

in which $F(h; t, s, n)$ is the hypergeometric cumulative distribution function

$$F(h; t, s, n) = \sum_{i=0}^{i=h} \frac{\binom{s}{i}\binom{t-s}{n-i}}{\binom{t}{n}} \quad (5)$$

We found $N = 4908$, used $T = 26515$ and retrieved S from the KEGG database (July, 2015). Table 1 shows the top 64 most enriched pathways—excluding the ones in organ functions and specific diseases.

3.5. Functional analysis

A more stringent criteria was used to select genes for functional annotation: a fold change >2 with a p-value <0.01. There were 1861 probes satisfied this criteria. To control the false discovery rate (FDR), the Benjamini-Hocheberg procedure [5] was applied to select further: for the FDR at level q, find the largest k such that

$$p_k \leq \frac{k}{m} q \quad (6)$$

then select $i = 1...k$, where p_k is the p-value of m genes with lowest p-values. For a FDR of 0.01, 1860 out 1861 probes were selected (Fig. 1d). Among those were 656 up-regulated and 391 down-regulated uniquely identified genes (see files mypup.txt.2x0.01p and mypdown.txt.2x0.01p). The generated gene list was functionally annotated using DAVID 6.7 (http://david.abcc.ncifcrf.gov/, [6]) with default setting (online file: myfa_table_all.txt.2x0.01p). The functional groups of genes were extracted from the annotated file using the corresponding terms (e.g. "signal transduction,") with our own script (online file: myfa.csh).

4. Results

4.1. Enriched expression in metabolic, cancer and PI3K signaling pathways

Metabolic Pathways, Pathways in Cancer and PI3K-Akt Signaling Pathway were the top three pathways enriched with the genes of significant expression change due to the CcO complex defect (Table 1). Among the three, Pathways in Cancer and PI3K-Akt Signaling Pathway had a lots of overlaps while they had little overlaps with

Table 1
Top 64 most enriched pathways in the C4KD cells compared to the control cells.
The top pathways were selected with the number of hits ≥ 20 and the p-value < 0.15.

Hits	Size	%	p-value	Kegg id	Name of pathway
330	1271	26	1.3e-11	01100	Metabolic pathways
127	397	32	6.4e-11	05200	Pathways in cancer
95	352	27	5.3-e05	04151	PI3K-Akt signaling pathway
74	232	32	6.3e-07	05203	Viral carcinogenesis
73	206	35	6.1e-09	05205	Proteoglycans in cancer
71	276	26	1.8e-03	05206	MicroRNAs in cancer
68	254	27	7.2e-04	04010	MAPK signaling pathway
66	208	32	3.0e-06	04510	Focal adhesion
64	170	38	3.4e-09	03013	RNA transport
64	218	29	6.3e-05	01130	Biosynthesis of antibiotics
64	235	27	6.3e-04	04144	Endocytosis
60	145	41	1.1e-10	03010	Ribosome
58	230	25	6.9e-03	04014	Ras signaling pathway
54	214	25	8.7e-03	04015	Rap1 signaling pathway
50	133	38	1.8e-07	03040	Spliceosome
49	118	42	5.5e-09	04919	Thyroid hormone signaling pathway
48	177	27	3.0e-03	05202	Transcriptional misregulation in cancer
45	168	27	5.1e-03	04141	Protein processing in endoplasmic reticulum
45	172	26	8.1e-03	04022	cGMP-PKG signaling pathway
45	179	25	1.7e-02	00230	Purine metabolism
44	198	22	1.1e-01	04062	Chemokine signaling pathway
43	139	31	2.7e-04	00190	Oxidative phosphorylation
43	143	30	5.4e-04	04120	Ubiquitin mediated proteolysis
41	142	29	1.7e-03	04910	Insulin signaling pathway
41	129	32	2.0e-04	04152	AMPK signaling pathway
41	174	24	5.5e-02	04145	Phagosome
40	181	22	1.3e-01	04020	Calcium signaling pathway
40	143	28	3.6e-03	04310	Wnt signaling pathway
39	159	25	3.5e-02	04921	Oxytocin signaling pathway
39	125	31	4.3e-04	04110	Cell cycle
38	154	25	3.4e-02	04390	Hippo signaling pathway
37	104	36	2.8e-05	00240	Pyrimidine metabolism
37	124	30	1.5e-03	04142	Lysosome
37	103	36	2.2e-05	04922	Glucagon signaling pathway
36	134	27	1.1e-02	04068	FoxO signaling pathway
35	122	29	4.0e-03	04722	Neurotrophin signaling pathway
35	115	30	1.3e-03	04114	Oocyte meiosis
34	140	24	5.2e-02	04530	Tight junction
33	140	24	7.8e-02	04550	Signaling pathways regulating pluripotency of stem cells
31	94	33	5.6e-04	00564	Glycerophospholipid metabolism
30	109	28	1.3e-02	04066	HIF-1 signaling pathway
29	101	29	8.1e-03	05231	Choline metabolism in cancer29
29	117	25	5.5e-02	01200	Carbon metabolism
28	124	23	1.5e-01	04071	Sphingolipid signaling pathway
27	87	31	3.3e-03	04540	Gap junction
26	88	30	7.9e-03	04512	ECM-receptor interaction
26	96	27	2.5e-02	03015	mRNA surveillance pathway
25	83	30	7.0e-03	03008	Ribosome biogenesis in eukaryotes
25	99	25	5.9e-02	04915	Estrogen signaling pathway
25	67	37	2.3e-04	04115	p53 signaling pathway
25	89	28	1.8e-02	04912	GnRH signaling pathway
25	82	30	5.9e-03	04210	Apoptosis
25	72	35	8.0e-04	04920	Adipocytokine signaling pathway
23	74	31	6.3e-03	04520	Adherens junction
23	87	26	4.3e-02	04012	ErbB signaling pathway
23	83	28	2.6e-02	03018	RNA degradation
23	82	28	2.2e-02	003320	PPAR signaling pathway
22	74	30	1.3e-02	04917	Prolactin signaling pathway
22	82	27	4.0e-02	04070	Phosphatidylinositol signaling system
22	66	33	2.9e-03	05230	Central carbon metabolism in cancer
21	82	26	6.9e-02	04350	TGF-beta signaling pathwa
20	79	25	8.2e-02	01230	Biosynthesis of amino acids
20	66	30	1.4e-02	00010	Glycolysis / Gluconeogenesis
20	61	33	5.4e-03	04150	mTOR signaling pathway

Metabolic Pathways (Fig. 2a). The 330 genes enriching Metabolic Pathways were distributed in different pathways of metabolism (Fig. 2b). Oxidative Phosphorylation was the leading one. Another enriched one was Glycolysis/Gluconeogenesis. Glycolysis is known to be responsible for energy generation if Oxidative Phosphorylation is interrupted. The 127 genes enriching Pathways in Cancer were sub-divided into many pathways (Fig. 2c). Interestingly, genes in PI3K-Akt Signaling Pathway accounted for one third overall and contributed about half to others except Wnt and Hippo signaling pathways.

The 95 genes enriching PI3K-Akt Signaling Pathway overlapped most significantly with pathways in cancer and also overlapped with additional signaling pathways (Fig. 2d). Especially interesting were AMPK and mTOR pathways, known to be activated during metabolic stress. Most of these pathways were among the top 64 enriched pathways and accounted for most of the signaling pathways of the top 64. One significant exception was Calcium Signaling Pathway (Table 1). It is significant because this pathway is involved in a unique retrograde signaling cascade responding to $[Ca^{2+}]_c$ elevation during disruptions of the mitochondrial electron transport chain [7]. We show in the following sections with specific expression changes that the defect in CcO complex caused metabolic shift to glycolysis, induced calcium dependent retrograde signaling, activated PI3K pathway and resulted in carcinogenesis.

4.2. Disruption of CcO complex leading to metabolic shift to glycolysis

The expression of Cox4i1 in the cells with Cox4i1 silenced by shRNA, referred as CcO4KD cells throughout this paper, was less than 5% of the control with scrambled shRNA (Fig. 3a). The mRNA expression levels of the irreversible glycolytic enzymes, Hexokinase (Hk1, Fig. 3b), Phosphofructokinae (Pfkm, Fig. 3c) and Pyruvate kinase (Pkm, Fig. 3d) had approximately two-folds increase. Fig. 3 also shows the mRNA expression levels of four other enzymes in the glycolytic pathway with the most fold-changes (Acss2, Adh1, Adh7 and Aldh2 in Fig. 3e to h). They were all up-regulated in CcO4KD cells and are downstream of glycolysis—important for processing pyruvate produced during glycolysis. In agreement with these data, CcO activity was reduced by about 90%, the Hk and Pfk activities increased about two folds, and glucose uptake was more than two-fold higher in CcO4KD cells [2]. These indicated that silencing Cox4i1 lead to the disruption of CcO activity and caused metabolic shift to glycolysis.

4.3. Activation of Calcium dependent retrograde signaling pathway

The mitochondrial stress and the loss of mitochondrial membrane potential were indicated by the enrichment of Calcium Signaling Pathway (Table 1) and in particular by a two-fold increase in the expression level of Ca^{2+} sensitive Calcineurin (Ppp3ca, Fig. 4a). This signal in response to sustained elevation of $[Ca^{2+}]_c$ had been shown to activate a set of stress responsive transcription factors: NFkB, NFAT and CREB [7]. This was consistent with the increased expression levels of Nfkb1, Nfkb2, Rela, Nfatc1, Nfatc3, Creb3l1 and Creb3l2 (Fig. 4b to h). In addition to those, this retrograde stress signaling induced increased expression of many genes involved in tumor progression. In particular, Tgfb1 and Mmp16 had 2 to 3 folds expression increase (Fig. 5a and b). In

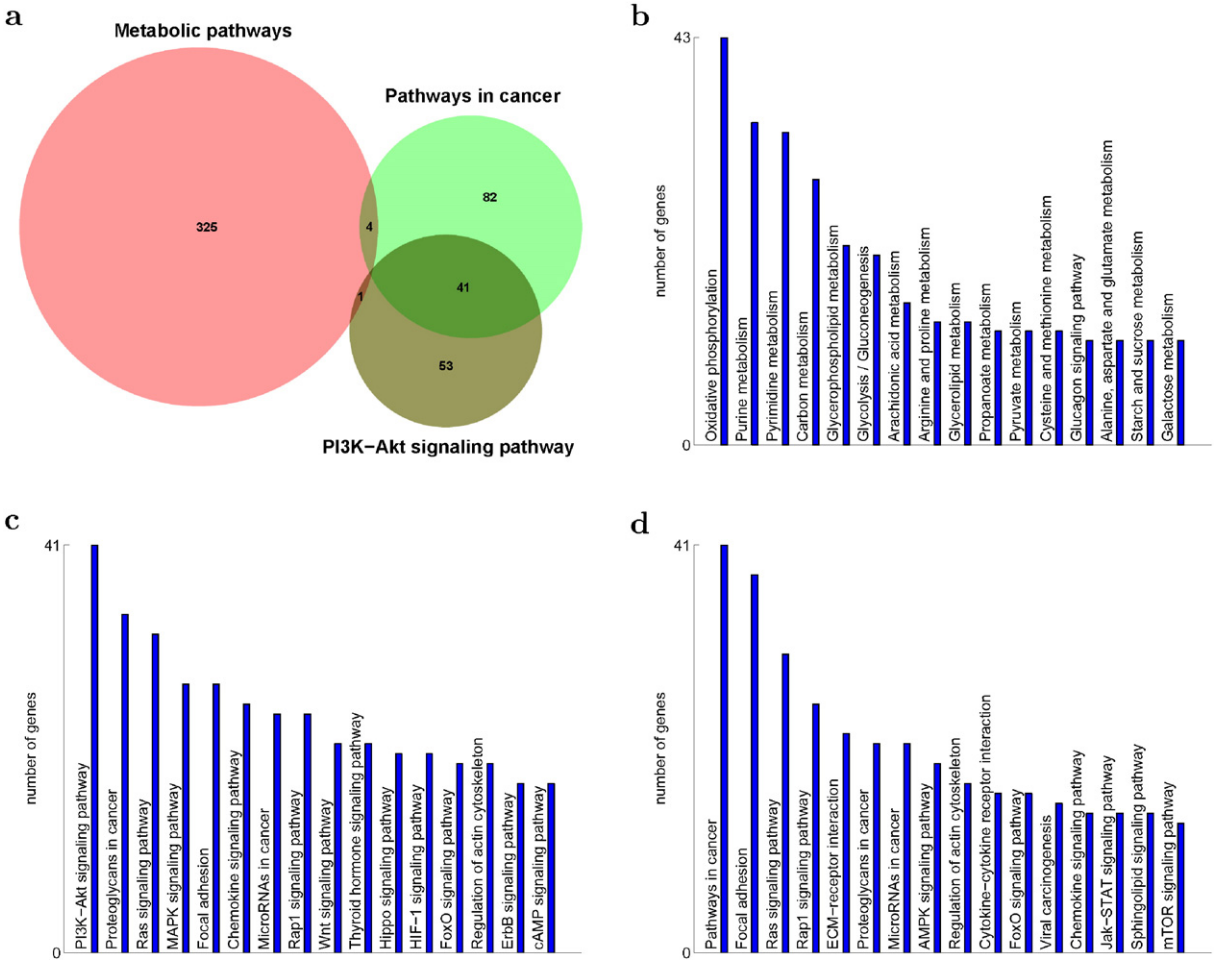

Fig. 2. Three major pathways of significantly regulated genes of CcO4KD cells—Metabolic Pathways, Pathways in Cancer and PI3K-Akt Signaling Pathway: **a**, overlaps between the three; **b**, Metabolic Pathways' overlaps with others; **c**, Pathways in Cancer's overlaps with others; **d**, PI3K-Akt Signaling Pathway's overlaps with others.

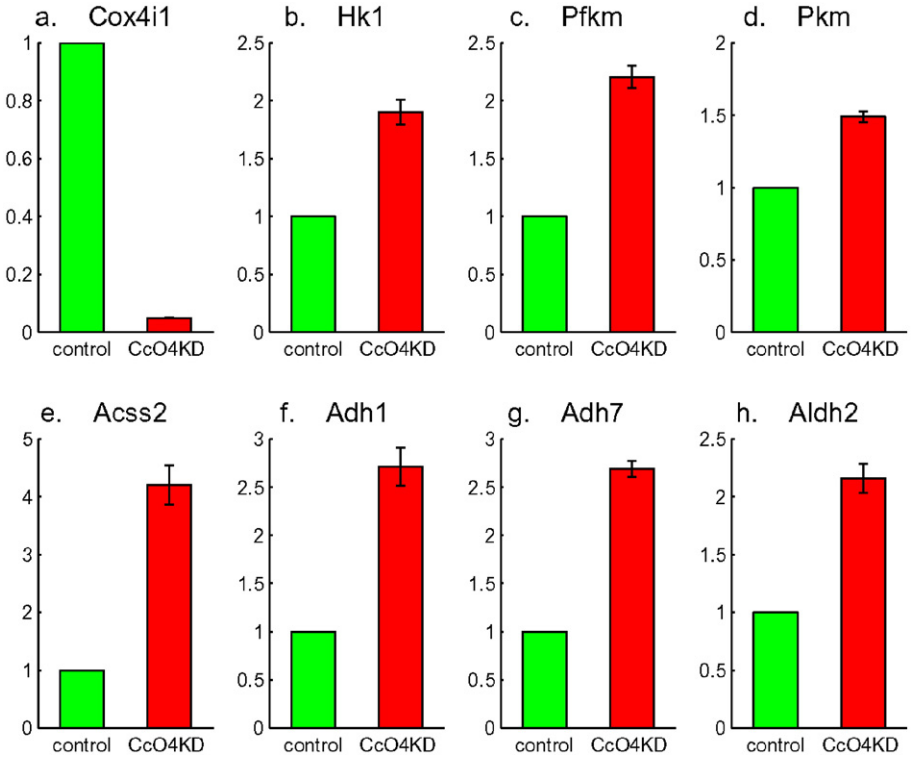

Fig. 3. Knock-down of the expression level of cytochrome c oxidase (Cox4i1 in **a**), and expression up-regulation of all three irreversible glycolytic enzymes Hexokinase (Hk1 in **b**), Phosphofructokinase (Pfkm in **c**) and Pyruvate Kinase (Pkm in **d**), as well as four other enzymes downstream of glycolysis: Acss2, Adh1, Adh7 and Aldh2 (**e**, **f**, **g** and **h**).

agreement with these data, Calcineurin activity increased three folds in CcO4KD cells; while for the cells further treated with BAPTA, a Ca^{2+} chelator, or FK506, a specific Calcineurin inhibitor, the up-regulation of Tgfb1 and Mmp16 was significantly attenuated and the glucose uptake was significantly inhibited comparing to untreated cells [2]. These indicated that the Calcineurin mediated retrograde signaling pathway played an important role in metabolic shift to glycolysis and carcinogenesis.

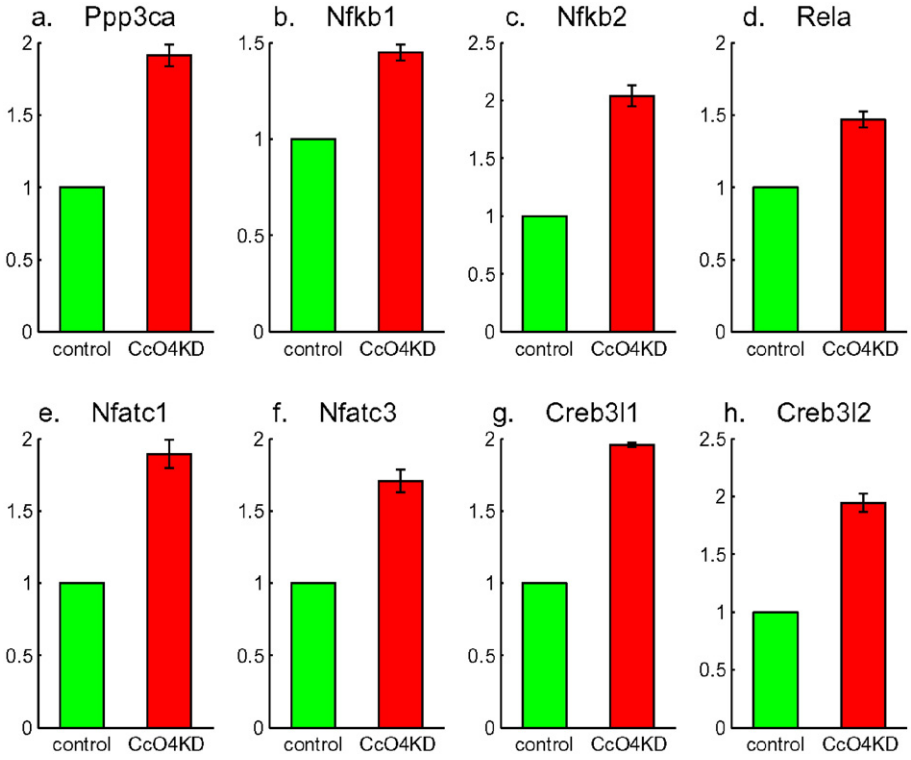

Fig. 4. Up-regulation of Calcineurin (Ppp3ca in **a**) and Calcineurin pathway: NFkB (Nfkb1 in **b**, Nfkb2 in **c** and Rela in **d**), NFAT (Nfatc1 in **e** and Nfatc3 in **f**), and CREB (Creb3l1 in **g** and Creb3l2 in **h**).

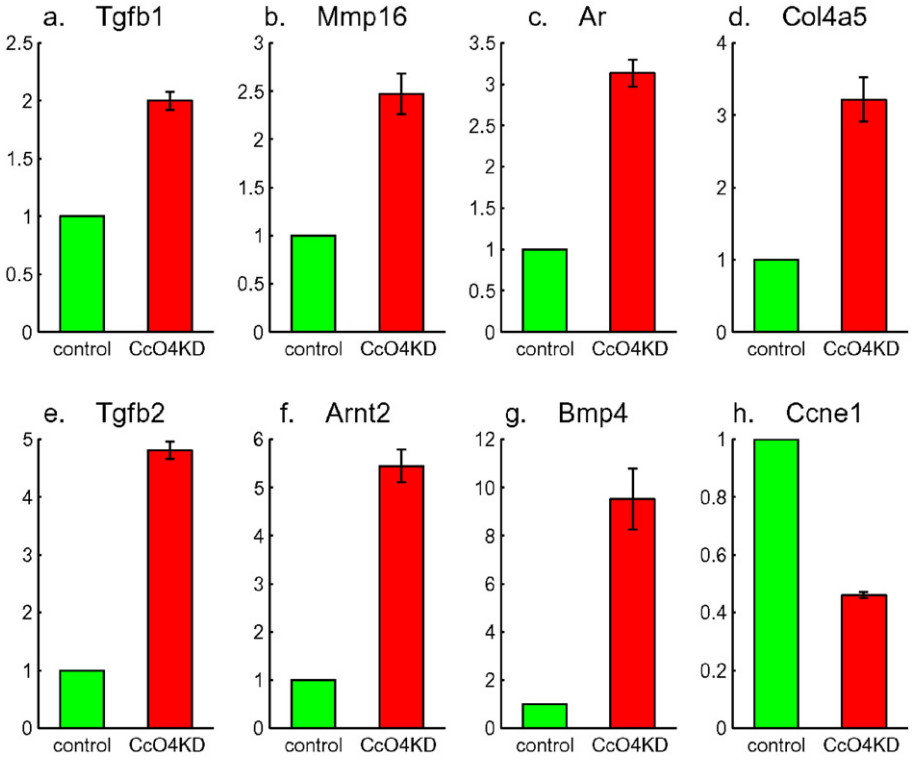

Fig. 5. Up-regulation of seven genes related to cancer: Tgfb1 in **a**, Mmp16 in **b**, Ar in **c**, Col4a5 in **d**, Tgfb2 in **e**, Arnt2 in **f** and Bmp4 in **g**. Down-regulation of one gene related to cancer: Ccne1 in **h**.

4.4. Activation of PI3-kinase pathway and carcinogenesis

The activation of PI3-kinase pathway was indicated by a two-fold increase in expression level of PI3-kinase—of both catalytic and regulatory subunits Pik3cb and Pik3r4 (Fig. 6a and b). It has been shown that this pathway is a major determinant of the glycolytic phenotype through Akt1 and Mtor signaling and subsequent downstream Hif1a transcription factor activation [8]. In addition to increased expression of Mtor and Hif1a (Fig. 6c and d) in CcO4KD cells, there were also increased expression levels for genes further down stream [9] of this pathway

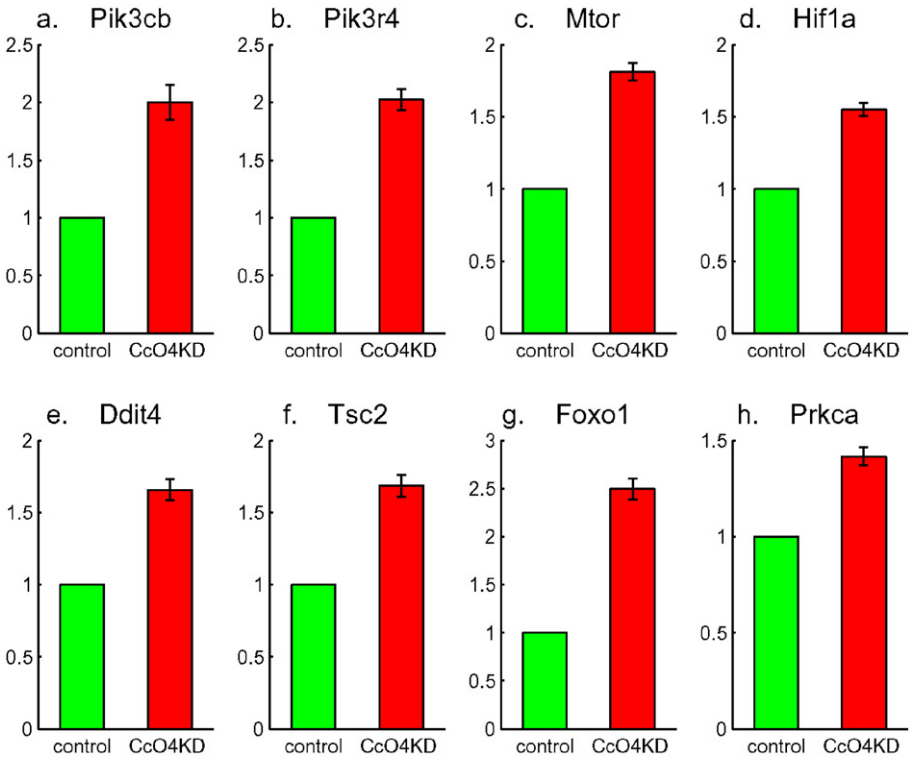

Fig. 6. Up-regulation of PI3-kinase (Pik3cb in **a** and Pik3r4 in **b**) and PI3-kinase pathway: Mtor in **c**, Hif1a in **d**, Ddit4 in **e**, Tsc2 in **f**, Foxo1 in **g**, and Prkca in **h**.

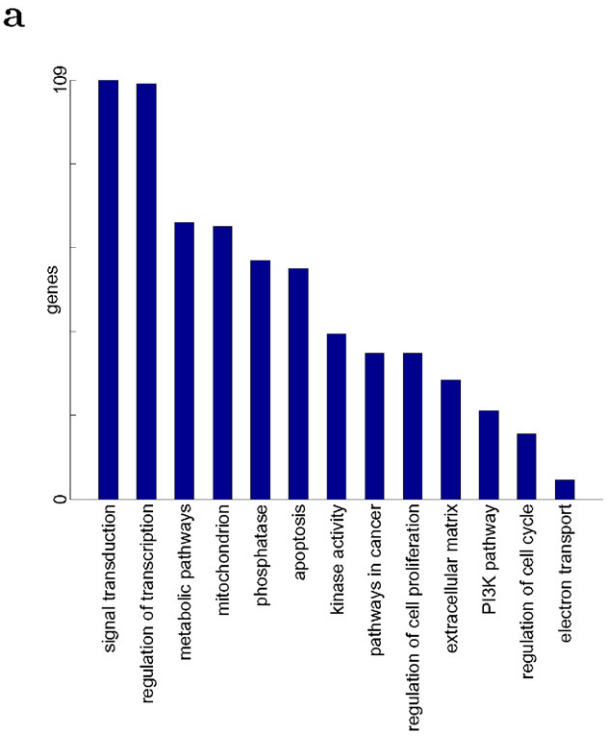

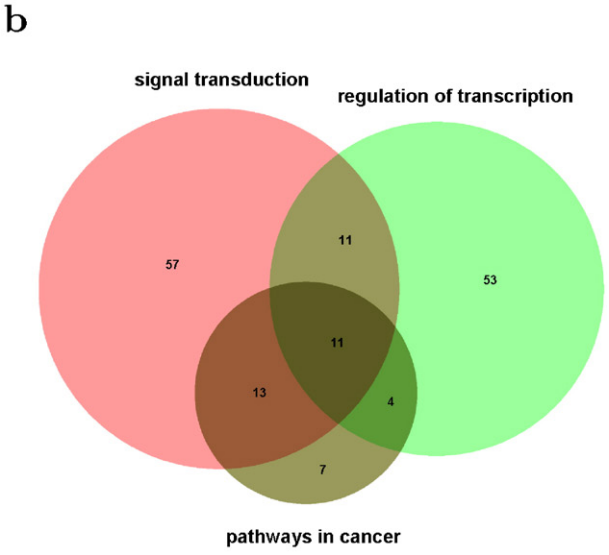

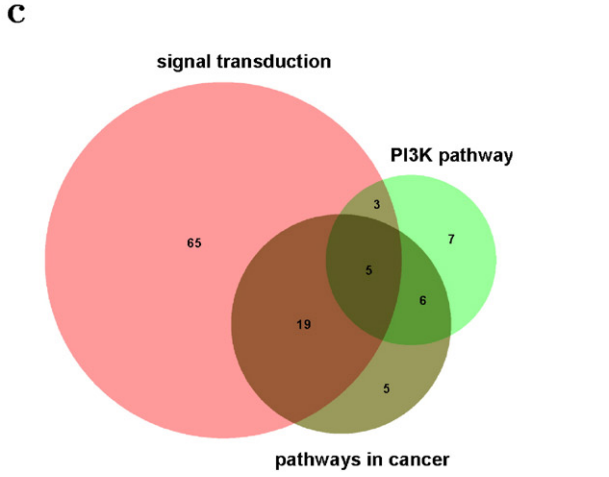

Table 2
38 significantly regulated genes in pathways in cancer. 35 were up-regulated in CcO4KD and only 3 were down-regulated (Ccne1, Ccne2 and Tceb1). The genes were selected with a fold change ≥2 and a *p*-value <0.01. The fold change is expressed in log_2 unit.

Symbol	Fold	*p*-Value	Entrez	Gene name
Ar	1.65	2e-04	11,835	Androgen receptor
Arnt2	2.45	1e-03	11,864	Aryl hydrocarbon receptor nuclear translocator 2
Bmp4	3.25	3e-04	12,159	Bone morphogenetic protein 4
Ccne1	−1.12	1e-03	12,447	Cyclin E1
Ccne2	−1.09	3e-04	12,448	Cyclin E2
Cebpa	1.54	2e-03	12,606	CCAAT/enhancer binding protein (C/EBP), α
Col4a2	1.45	2e-04	12,827	Collagen, type IV, α 2
Col4a5	1.69	1e-03	12,830	Collagen, type IV, α 5
Col4a6	1.02	1e-04	94,216	Collagen, type IV, α 6
Dapk2	1.45	1e-03	13,143	Death-associated protein kinase 2
Ep300	1.03	2e-05	328,572	E1A binding protein p300
Figf	1.31	1e-03	14,205	c-fos induced growth factor
Foxo1	1.32	1e-03	56,458	Forkhead box O1
Fzd4	1.08	4e-03	14,366	Frizzled homolog 4 (Drosophila)
Fzd6	1.56	4e-03	14,368	Frizzled homolog 6 (Drosophila)
Gli2	1.07	5e-03	14,633	GLI-Kruppel family member GLI2
Jak1	1.02	2e-05	16,451	Janus kinase 1
Kitl	1.46	2e-03	17,311	Kit ligand
Lama2	1.49	1e-04	16,773	Laminin, α 2
Lamb3	1.35	6e-04	16,780	Laminin, β 3
Lamc1	1.18	3e-05	226,519	Laminin, γ 1
Met	1.13	2e-03	17,295	Met proto-oncogene
Ncoa4	1.05	2e-04	27,057	Nuclear receptor coactivator 4
Nfkb2	1.03	9e-04	18,034	Nuclear factor of κ light polypeptide gene enhancer in B cells 2
Pdgfb	1.74	8e-04	18,591	Platelet derived growth factor, B polypeptide
Ppard	1.15	9e-04	19,015	Peroxisome proliferator activator receptor delta
Rxra	1.03	2e-04	20,181	Retinoid X receptor α
Stat1	1.23	1e-03	20,846	Signal transducer and activator of transcription 1
Stat5a	1.02	1e-04	20,850	Signal transducer and activator of transcription 5A
Tceb1	−1.09	1e-03	67,923	Transcription elongation factor B (SIII), polypeptide 1
Tcf7	1.16	6e-03	21,414	Transcription factor 7, T cell specific
Tcf7l2	1.05	4e-05	21,416	Transcription factor 7 like 2, T cell specific, HMG box
Tgfb1	1.00	6e-04	21,803	Transforming growth factor, β 1
Tgfb2	2.27	1e-05	21,808	Transforming growth factor, β 2
Tgfbr2	1.36	4e-05	21,813	Transforming growth factor, β receptor II
Wnt10a	1.58	9e-04	22,409	Wingless related MMTV integration site 10a
Wnt4	1.16	7e-03	22,417	Wingless-related MMTV integration site 4
Wnt7b	1.40	3e-04	22,422	Wingless-related MMTV integration site 7B

including Redd1(Ddit4), Tsc2, Foxo1 and PKCα(Prkca) (Fig. 6e to h) as well as other genes related to pathways in cancer (Fig. 5). Aerobic glycolysis supports various biosynthetic pathways and, consequently, the metabolic requirements for proliferation. Consistent with this, the CcO4KD cells developed anchorage independent growth, an important hallmark of malignant cells, and further treatment with Wortmannin, a PI3-kinase inhibitor, attenuated the glucose uptake and inhibited the colony formation of those cells [2]. These indicated that the PI3-kinase pathway played a crucial role in metabolic shift to glycolysis and in tumor progression.

4.5. Oncogenes enriched transcription profiles

Bmp4, Arnt2, Tgfb2, Col4a5 and Ar (shown in Fig. 5c to g) were the five most up-regulated genes in Pathways in Cancer. Ccne1 (shown in

Fig. 7. Functional groups of significantly regulated genes of CcO4KD cells: **a**, the number of genes with significant fold-changes in different functional groups; **b**, the Venn diagrams of up-regulated genes in signal transduction (pink), regulation of transcription (green) and pathways in cancer (brown); **c**, the Venn diagrams of up-regulated genes in signal transduction (pink), PI3K pathway (green) and pathways in cancer (brown).

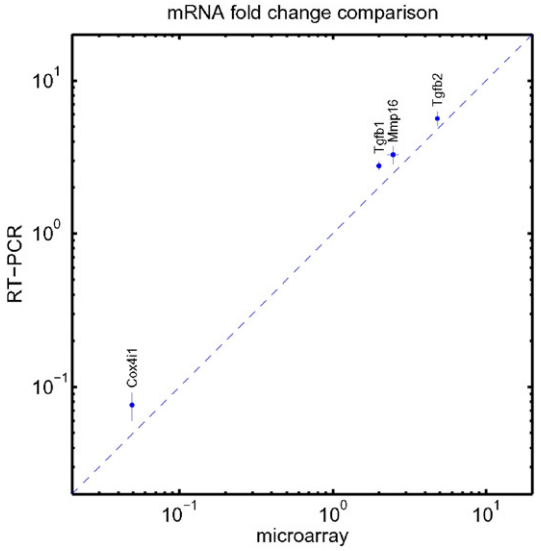

Fig. 8. The comparison between the expression fold changes of four genes from microarray and those measured by RT-PCR in a log-log plot. The straight line lies where they are equal.

Fig. 5h) was the most down-regulated gene in Pathways in Cancer. Col4a5 and Ccne1 are in PI3K-Akt Pathway and their corresponding up and down regulation are consistent with their role in cancers. Furthermore, Ar, Bmp4 and Tgfb2 are involved in signal transduction and Ar, Arnt2 and Bmp4 are involved in regulation of transcription. To gain additional understanding of functional roles of the most significantly regulated genes of CcO4KD cells, we further narrowed down the list of genes and did functional annotation of the list. There were 1047 genes with 2-fold or more expression change and p-value less than 0.01. The distribution of those genes in the three dominate pathways and 10 different functional groups is shown in Fig. 7a. Among those were 38 significantly regulated genes in Pathways in Cancer (enrichment p-value less than 10^{-6}). Table 2 shows the fold changes and the p-values of the 38 genes. 35 genes in Pathways in Cancer were up-regulated (enrichment p-value less than 10^{-5}). 24, 15 and 11 of these up-regulated genes in pathways in cancer are in functional groups of signal transduction, regulation of transcription and PI3K pathway, respectively. There were extensive overlaps (11) between those in signal transduction and regulation of transcription (Fig. 7b). There were also overlaps (5) between those in signal transduction and PI3K pathway (Fig. 7c). There was only one (Rxra) overlap between those in regulation of transcription and PI3K pathway. Only two genes (Dapk2 and Ncoa4) in pathways in cancer were not in any of the other three functional groups. Interestingly, none of genes in pathways in cancer was in metabolic pathway. It appears that CcO defects induced Calcineurin/PI3K retrograde signaling which in turns induced up-regulation of genes involved in signal transduction and regulation of transcription, up-regulation of genes related to pathways in cancer, and carcinogenesis.

5. Discussion

The whole genome microarray analysis of the knockdown and control cells gave the insight into the magnitude of systematic changes of gene expressions and also enabled the global analysis of pathways and functional groups of many genes efficiently. It is interesting to know the accuracy of individual fold change of gene expression estimated from the experimental array. For some of the genes, the relative mRNA levels were also measured by RT-PCR [2]. Fig. 8 shows the comparison between the results of microarray and RT-PCR. The agreement is quite good. The that fold change estimated by the array is slightly on the conservative side. This gave confidence to use the array not only for the global analysis but also for measuring relative change of individual gene's mRNA level.

The pathway analysis also indicated that PPAR (PGC-1α) signaling pathway was activated. PGC-1α is another regulator of mitochondrial biogenesis and function. It has been shown that PGC-1α has a positive

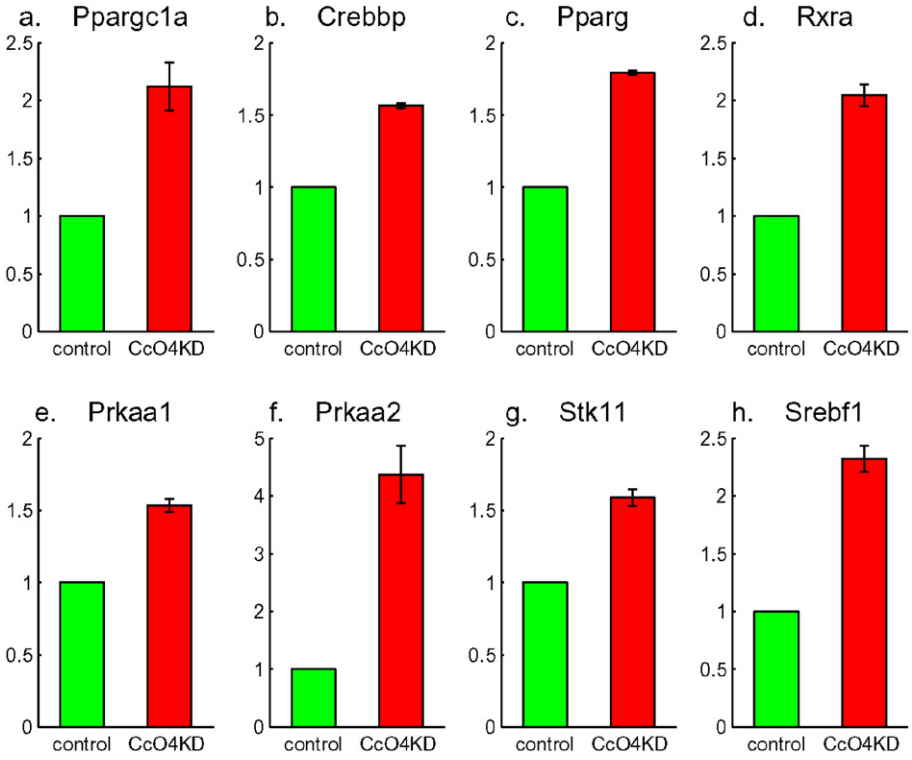

Fig. 9. Up-regulation of PGC-1α (Ppargc1a in **a**) and its interaction partners: Crebbp in **b**, Pparg in **c**, and Rxra in **d**. Up-regulation of AMPK (Prkaa1 in **e** and Prkaa2 in **f**), its upstream regulator LKB1 (Stk11 in **g**) and a downstream gene Srebf1 in **h**.

feedback to one of its upstream regulator: Calcineurin [10]. This protein can interact with, and regulate the activities of, cAMP response element-binding protein (CREB). Fig. 9a to d shows the up-regulation of PGC-1α (Ppargc1a) and its interaction partners Crebbp, Pparg, and Rxra. Another important pathway activated was the AMP-activated protein kinase (AMPK) signaling pathway. AMPK plays an important role in insulin signaling, glucose uptake, and energy homeostasis and is involved in PGC-1α-mediated mitochondrial biogenesis. The microarray analysis indicated up-regulation of AMPK (Prkaa1 and Prkaa2 in Fig. 9e and f) and its up-stream regulator LKB1 (Stk11, Fig. 9g) as well as two downstream genes (Srebf1, Fig. 9h; and Tsc2, Fig. 6f). This is puzzling since AMPK is supposed to down-regulated Srebf1 and Tsc2 and to be a metabolic checkpoint to control cell proliferation when activated under energy stress. But it was not doing any of those in CcO4KD cells. The role of AMPK pathway in Cox4i1 knockdown needs to be studied further.

Our physiological experiments have shown that CcO dysfunction is a possible biomarker for cancer progression in digestive diseases such as esophageal tumors [2]. It will be very interesting to conduct a whole genome expression analysis on such tumors and to compare the results with those presented in this paper. Such comparison will help to further understand the pathways of this type of tumor progression and to find possible pathway-based methods of diagnosis and treatment.

Acknowledgments

This work was supported by NIH grant CA-22762, NIH/NIDDK Center grant P30DK050306, and a grant from Research Foundation, University of Pennsylvania.

References

[1] R.A. Irizarry, B. Hobbs, F. Collin, Y.D. Beazer-Barclay, K.J. Antonellis, U. Scherf, T.P. Speed, Exploration, normalization, and summaries of high density oligonucleotide array probe level data. Biostatistics 4 (2) (2003) 249–264.
[2] S. Srinivasan, M. Guha, D.W. Dong, K.A. Whelan, G. Ruthel, Y. Uchikado, S. Natsugoe, H. Nakagawa, N.G. Avadhani, Disruption of cytochrome c oxidase function induces Warburg effect and metabolic reprogramming. Oncogene (2015)http://dx.doi.org/10.1038/onc.2015.227 (in press).
[3] G.D. Ruxton, The unequal variance t-test is an underused alternative to Student's t-test and the Mann-Whitney U test. Behav. Ecol. 17 (2006) 688–690.
[4] M. Kanehisa, S. Goto, S. Kawashima, Y. Okuno, M. Hattori, The KEGG resource for deciphering the genome. Nucleic Acids Res. 32 (1) (2004) D277–D280.
[5] Y. Benjamini, Y. Hochberg, Controlling the false discovery rate: a practical and powerful approach to multiple testing. J. R. Stat. Soc. Ser. B 57 (1) (1995) 289–300.
[6] D.W. Huang, B.T. Sherman, R.A. Lempicki, Bioinformatics enrichment tools: paths toward the comprehensive functional analysis of large gene lists. Nucleic Acids Res. 37 (1) (2009) 1–13.
[7] M. Guha, S. Srinivasan, G. Biswas, N.G. Avadhani, Activation of a novel calcineurin-mediated insulin-like growth factor-1 receptor pathway, altered metabolism, and tumor cell invasion in cells subjected to mitochondrial respiratory stress. J. Biol. Chem. 282 (19) (2007) 14536–14546.
[8] A.L. Simons, K.P. Orcutt, J.M. Madsen, P.M. Scarbrough, D.R. Spitz, Oxidative stress in cancer biology and therapy. Humana Press, 2012 21–46.
[9] J. Brugarolas, K. Lei, R.L. Hurley, B.D. Manning, J.H. Reiling, E. Hafen, L.A. Witters, L.W. Ellisen, J.W.G. Kaelin, Regulation of mTOR function in response to hypoxia by REDD1 and the TSC1/TSC2 tumor suppressor complex. Genes Dev. 18 (23) (2004) 2893–2904.
[10] S. Summermatter, R. Thurnheer, G. Santos, B. Mosca, O. Baum, S. Treves, H. Hoppeler, F. Zorzato, C. Handschin, Remodeling of calcium handling in skeletal muscle through PGC-1α: impact on force, fatigability, and fiber type. Am. J. Physiol. Cell Physiol. 302 (1) (2012) C88–C99.